

# Photoluminescence characteristics of $Y_3Al_5O_{12}:Tb^{3+}$ phosphors synthesized using the combustion method

Hyun-ho Kwak · Se-Jun Kim · Hyon-Hee Yoon ·  
Sang-Joon Park · Hyung-wook Choi

Received: 25 May 2007 / Accepted: 18 March 2008 / Published online: 17 April 2008  
© Springer Science + Business Media, LLC 2008

**Abstract** For this study, terbium-doped yttrium aluminum garnet (YAG:Tb) phosphor powders were prepared via the combustion process using the 1:1 ratio of metal ions to reagents. The characteristics of the synthesized nano powder were investigated by means of X-ray diffraction (XRD), scanning electron microscope (SEM), and photoluminescence. Single-phase cubic YAG:Tb crystalline powder was obtained at 800 °C by directly crystallizing it from amorphous materials, as determined by XRD techniques. There were no intermediate phases such as yttrium aluminum perovskite ( $YAlO_3$ ) and yttrium aluminum monoclinic ( $Y_4Al_2O_9$ ) observed in the sintering process. The SEM image showed that the resulting YAG:Tb powders had uniform sizes and good homogeneity. With the increase in the sintering temperature, the grain size increased. The photoluminescence spectra of the YAG:Tb nanoparticles were investigated to determine the energy level of electron transition related to luminescence processes. There were three peaks in the excited spectrum, and the major one was a broad band of around 274 nm. Also, the YAG:Tb nanoparticles showed two emission peaks in the range of 450×500 and 525×560 nm, respectively, and had maximum intensity at 545 nm.

**Keywords** YAG · Combustion · Phosphor · Luminescence

H.-h. Kwak · S.-J. Kim · H.-w. Choi (✉)  
Department of Electrical Engineering, Kyungwon University,  
San 65, Bokjung-dong, Sujung-gu,  
Seongnam, Gyunggi-do 461-701, Republic of Korea  
e-mail: chw@kyungwon.ac.kr

H.-H. Yoon · S.-J. Park  
Department of Chemical and Bio Engineering,  
Kyungwon University,  
San 65, Bokjung-dong, Sujung-gu,  
Seongnam, Gyunggi-do 461-701, Republic of Korea

## 1 Introduction

Yttrium aluminum garnet ( $Y_3Al_5O_{12}$ , YAG) is an advanced ceramic with interesting optical and mechanical properties [1]. A host crystal with an yttrium aluminum garnet structure has the advantage of a relatively stable lattice and large thermal conductivity. Thus, YAG can be used as the host lattice for a number of rugged phosphor systems [2]. It is an important crystal for fluorescence and solid-state lasers.

Tb-activated YAG phosphor has luminescence properties that are fairly insensitive to temperature variations, and it shows tendency to saturate at high current excitations. Furthermore, YAG:Tb is a characteristic narrowband phosphor suitable for contrast-enhanced display applications in high ambient illumination conditions [3]. Hence, YAG:Tb is one of the promising phosphor candidates that may be used in projection cathode ray tubes, field emission display, and scintillation and electroluminescence applications [4]. To enhance the brightness and resolution of these displays, it is important to develop phosphors with high quantum efficiency, controlled morphology, and small particle sizes. It has been found that the luminescence efficiency of YAG:Tb phosphor depends on the synthesis method, which can lend itself to the formation of single-phase YAG.

Commercial phosphors such as YAG:Tb are typically prepared via the conventional solid-state reaction at high temperatures (>1400 °C) [5–8].

However, the conventional process has some disadvantages such as high temperature firing for extended times and repeated grinding and milling for mechanical particle-size reduction followed by re-firing. While high temperature firing is necessary for crystallization, it can introduce defects and impure phases. Furthermore, grinding and milling also introduce defects that can lower the overall brightness and

efficiency of these phosphors. The physical mixture of the solid precursors used for the solid-state reaction has an inherent limit for obtaining a compositionally homogeneous product. For phosphor applications, it is desirable to have a fine particle size for high resolution, and chemical purity for optimum chromaticity and brightness [1]. To overcome the disadvantages of the solid-state reaction process, several wet chemical synthesis techniques have also been used to prepare YAG powders [9–11], such as the sol-gel, coprecipitation, and solvothermal methods. These methods have the advantages of fine homogeneity, high reactivity of starting materials, and lower sintering temperatures. However, they are time-consuming and require strict techniques.

In contrast, the combustion method is quite simple, and the combustion reaction lasts only a few seconds. This process perfectly combines the merits of the sol-gel process and the low-temperature combustion process. This novel sol-gel combustion synthesis has the advantages of inexpensive precursors, convenient process control, and large mass production [9, 12, 13].

In this study, Tb-doped YAG phosphor precursors were synthesized using the combustion method. The luminescence, formation process, and structure of phosphor powders were evaluated using X-ray diffraction (XRD), scanning electron microscope (SEM) and photoluminescence (PL) through the sintering temperature.

## 2 Experimental

$\text{Y}(\text{NO}_3)_3 \cdot 6\text{H}_2\text{O}$  (99.9%, Aldrich),  $\text{Al}(\text{NO}_3)_3 \cdot 9\text{H}_2\text{O}$  (99.997%, Aldrich),  $\text{Tb}(\text{NO}_3)_3 \cdot 6\text{H}_2\text{O}$  (99.9%, Aldrich), and citric acid ( $\text{C}_6\text{H}_8\text{O}_7 \cdot \text{H}_2\text{O}$ , Aldrich) were used as starting materials in this study, citric acid was the source of citrate anion that was used as both chelating agent to metal cations and fuel for the combustion.

Yttrium nitrate, aluminum nitrate, and terbium nitrate were combined to yield a composition with the general formula  $(\text{Y}_{1-x}\text{Tb}_x)_3\text{Al}_5\text{O}_{12}$ , with  $x=0.05$ . The ratio of all the metal ions to the citric acid used in this study was 1:1.

$\text{Y}(\text{NO}_3)_3 \cdot 6\text{H}_2\text{O}$ ,  $\text{Al}(\text{NO}_3)_3 \cdot 9\text{H}_2\text{O}$ , and  $\text{Tb}(\text{NO}_3)_3 \cdot 6\text{H}_2\text{O}$  were dissolved in deionized water. Afterwards, the solution was stirred using a magnetic bar in air for 20 min. Also, the citric acid was dissolved in deionized water. Then the citric acid solution was heated at 80 °C and continuously stirred using a magnetic bar.

Next, the metal solution was dropped into the citric acid solution at a rate of 1.6 ml/min, after which the solution was heated for 2 h at 80 °C. At the same time, we perform the experiment using reflux system to preserve the concentrations. Figure 1 is photograph of reflux system.

The solution was then rapidly heated to 200 °C for combustion. The color of the solution changed to bright



**Fig. 1** Reflux system for preserving the concentration

yellow. After a few minutes, the solution started combusting into brown gas. Finally, the precursor was produced. The precursor was dried in air and then sintered at 600–1400 °C for 2 h using an alumina crucible on a box furnace.

The crystalline development of the product was identified by XRD analysis (model D/MAX-2200) with  $\text{CuK}\alpha$ -radiation in the range of  $2\theta = 20^\circ$ – $80^\circ$ . The particle size and shape of the powders were observed with a Hitachi SEM (S4700). The excitation and emission spectra were obtained with a JASCO FP-6200 fluorescence spectrophotometer.

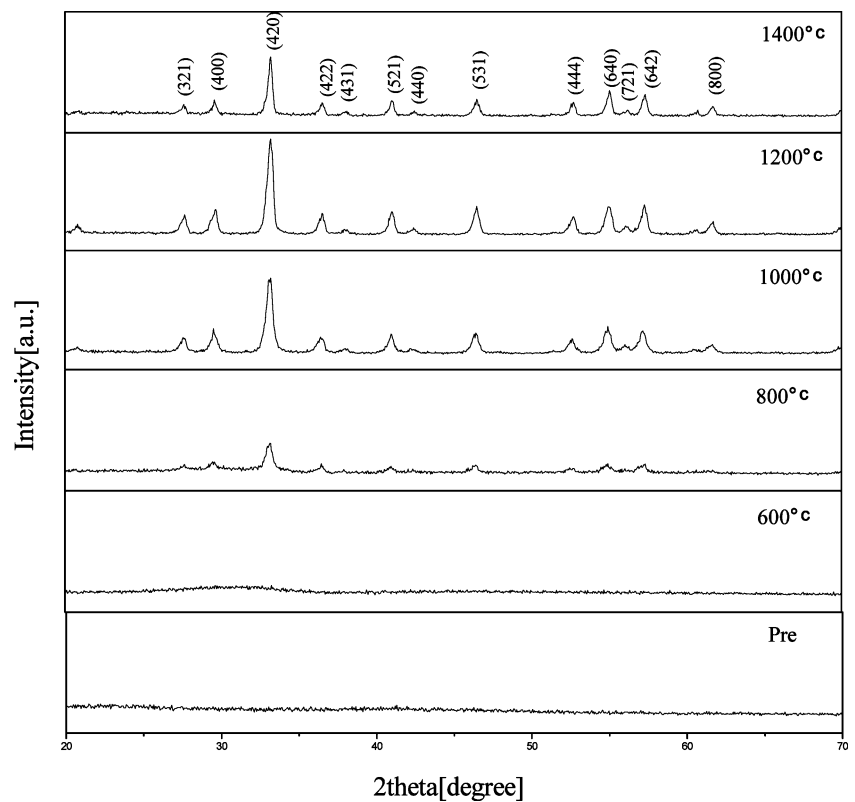
## 3 Results and discussion

The crystal chemical purity of the materials was checked via XRD. The XRD patterns of the YAG:Tb phosphor at various temperatures are shown in Fig. 2.

Because no obvious diffraction peaks were observed, it can be concluded that the precursor was amorphous and remained amorphous up to 600 °C. The various YAG peaks, with the (420) main peak, appeared at the sintering temperature of 800 °C. However, the crystal property was not perfected.

At above 1000 °C, more defined peak shapes with stronger intensities were observed, indicating the crystallite

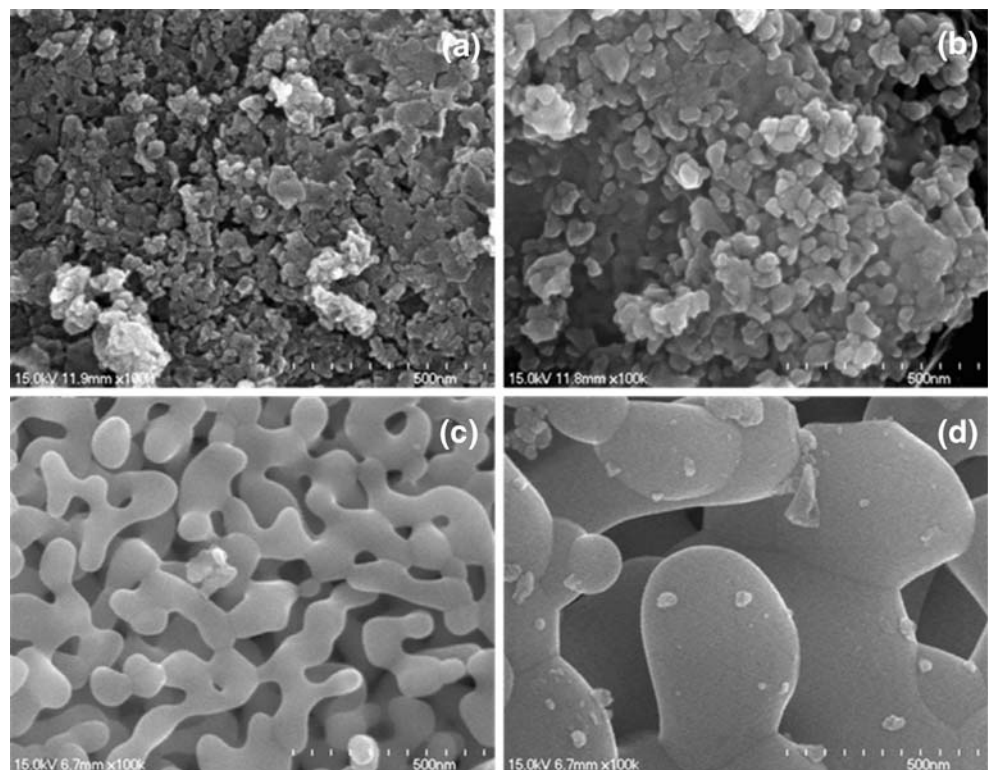
**Fig. 2** XRD patterns of the precursor and the YAG:Tb powders sintered at different temperatures



growth of the YAG powders as the temperature increased. The phase evolution shown by XRD indicates that YAG was the only phase detected during the heat treatment. It can be concluded that YAG appears to crystallize directly

from the amorphous precursor without the formation of any intermediate phase, indicating the higher cation homogeneity of the precursor. This result differs from those of other wet-chemical methods [14–16], in which yttrium aluminum

**Fig. 3** SEM images of the YAG:Tb phosphor sintered at (a) 800, (b) 1000, (c) 1200, and (d) 1400 °C



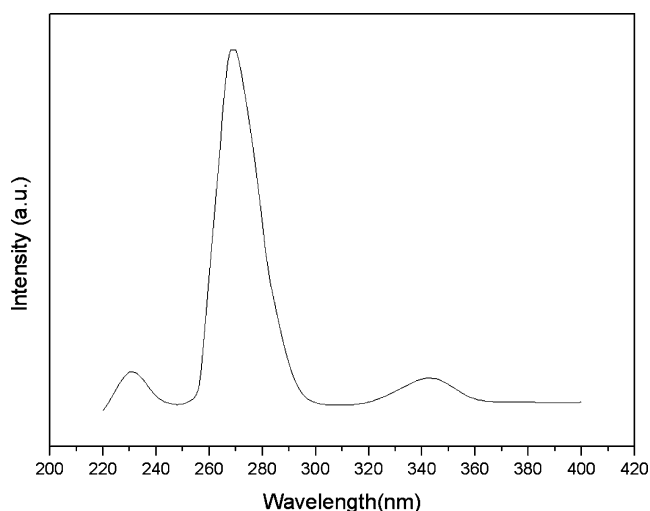


**Fig. 4** Excitation spectra of the Tb<sup>3+</sup> 545 nm emission in YAG:Tb

perovskite (YAP) and yttrium aluminum monoclinic (YAM) usually appear as intermediate phases. At 1200 °C, the diffraction peaks become stronger than peaks of sintered 1000 °C. But, we could be know that Full-Width at Half-Maximum decrease. We know that the grain size is more larger by means of the Scherrer formula. Through the diffraction peaks of sintered 1400 °C, We can anticipate that the grains of the YAG:Tb powder aggregated.

Figure 3 shows the SEM images of the YAG:Tb phosphor as a function of the sintering temperature for 2 h. The surface morphologies of the sintered powder at 800 °C had rough shapes. With increased sintering temperature, the phosphor particles became large and spherical. Uniform and spherical particles of YAG:Tb phosphor with homogeneous structures were obtained using the combustion method at 800 °C. The mean size of the particles measured from the SEM image was less than the 50 nm. It was known that the use of spherical phosphor particles would increase the screen brightness and improve resolution because of the lower scattering of the evolved light and the higher packing density compared with the irregularly shaped particles obtained using conventional methods. On one hand, the particle size reached nearly 500 nm at 1400 °C. It was also seen that the grain size was slow at a low sintering temperature and rapid above 1000 °C. Moreover, the grains of the YAG:Tb powder aggregated at a high temperature.

Figure 4 shows the excitation spectrum of the Tb<sup>3+</sup> 545 nm emission in YAG:Tb. The excitation spectrum consisted of three bands: a strong excitation band at about 274 nm and two weak excitation bands at 231 and 343 nm, respectively. All these corresponded to the Tb<sup>3+</sup> 4f–5d absorption.

The PL spectra of the YAG:Tb that was heat-treated at different temperatures and excited with ultraviolet ( $\lambda = 274$  nm) are shown in Fig. 5. At the sintering temperature

range of 600–1400 °C, the emission spectra had two peaks, at 490 and 544 nm, respectively. These two peaks that were above 480 nm were from the  $^5D_4 \rightarrow ^7F_j (j = 6, \dots, 0)$  transition [3]. The green emission started to dominate, and the maximum brightness was at 544 nm. This result was in good agreement with the results of the study conducted by Ohno and Marija [5, 17].

On the other hand, the luminescence spectra and the intensity did not change significantly at the sintering temperature range of 800–1200 °C, which can be understood by considering the purity of the single-phase cubic YAG and its well-defined crystallinity, even when the precursor was sintered at a low temperature. However, the emission spectra intensity of the YAG:Tb phosphor at 1400 °C decreased. This was because the high temperature condensed the particle [18].

#### 4 Conclusions

Nanoparticles of YAG:Tb phosphor were synthesized using a combustion method that was much lower than that adopted by the conventional solid-state method. Moreover, the XRD pattern shows that single-phase cubic YAG:Tb is formed by direct crystallization from amorphous materials, and no intermediate phase (YAM and YAP) was observed. Also, the (420) main peak appeared at the sintering temperature of 800 °C, which was in good agreement with the result of the JCPDS diffraction file 33-0040.

The SEM images with increased sintering temperature showed that the precursor directly transformed the pure YAG and that the phosphor particles were regularly spherical, with a size of about 50 nm at 800 °C. Above 1000 °C, the phosphor particles were much larger than 50 nm.

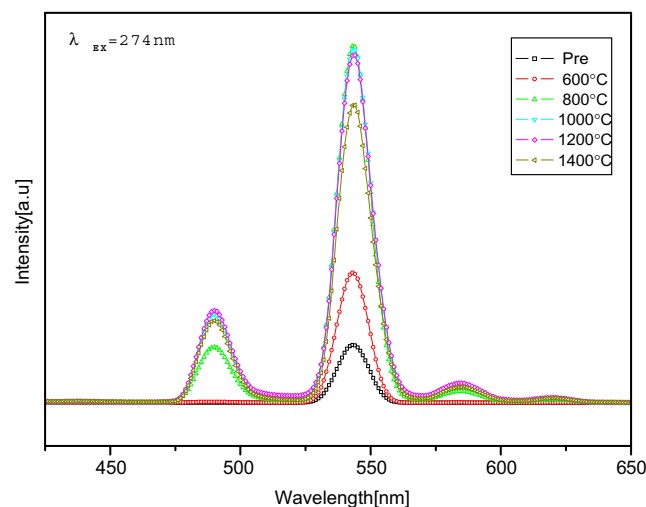


**Fig. 5** Emission spectra of the precursor and the YAG:Tb powders sintered at different temperatures

The fluorescence spectra were dominated by the  ${}^5D_4$  emission. With increased sintering temperature, the emission peak dramatically increased due to the good crystal property. However, the PL spectra shape and intensity did not change significantly between 800 and 1200 °C, indicating the purity of the single-phase cubic YAG and its high crystallinity, even at a low sintering temperature.

We perform the experiment using reflux system to preserve the concentrations for compounding metal ions. As a result, we prepared phosphor that has grain size of under 50 nm and excellent photoluminescence characteristic below 1000 °C of sintered temperature.

**Acknowledgements** This work was supported by the Kyunwon University Regional Innovation Center.

## References

1. B. Hoghooghi et al., *Mater. Chem. Phys.* **38**, 175–180 (1994)
2. J.M. Robertson, M.W. van Tol, *Appl. Phys. Lett.* **37**, 471 (1980)
3. G. Blasse, A. Bril, *Appl. Phys. Lett.* **11**, 53 (1967)
4. J. Ly, M. Prubhu, J. Xu, *Appl. Phys. Lett.* **77**, 707 (2000)
5. K. Ohno, T. Abe, *J. Electrochem. Soc.* **133**, 538 (1986)
6. K. Ohno, T. Abe, *J. Electrochem. Soc.* **134**, 2072 (1987)
7. J.S. Abell, I.R. Harris, B. Cockayne, B. Lent, *J. Mater. Sci.* **9**, 527 (1974)
8. D.R. Messier, G.E. Gazaa, *J. Am. Ceram. Soc.* **51**, 692 (1972)
9. S.K. Ruan, J.G. Zhou, A.M. Zhony et al., *J. Alloys Compounds* **72**, 275–277 (1998)
10. Y.C. Kang, I.W. Lenggoro, S.B. Park, K. Okuyama, *Master. Res. Bul.* **35**, 789 (2000)
11. S.K. Shi, J.Y. Wang, *J. Alloys Compounds* **82**, 327 (2001)
12. Y.C. Kang, I.W. Lenggoro, S.B. Park, K. Okuyama, *J. Phys. Chem.* **60**, 1855 (1999)
13. X. Li, H. Liu, J. Wang, H. Cui, F. Han, *Mater. Res. Bul.* **39**, 1923 (2004)
14. K.R. Han, H.J. Koo, C.S. Lim, *J. Am. Ceram. Soc.* **82**(6), 1598–1600 (1999)
15. J.G. Li, T. Ikegami, J.H. Lee, T. Mori, *J. Am. Ceram. Soc.* **83**(4), 961–963 (1999)
16. N. Matsushita, N. Tsuchiya, K. Nakatsuka, T. Yanagitani, *J. Am. Ceram. Soc.* **82**(8), 1977–1984 (1999)
17. J.Y. Choe, D. Ravichandran, S.M. Blomquist, K.W. Kirchner et al., *J. Lumin.* **93**, 119 (2001)
18. Z. Yang, X. Li, Y. Yang, Z. Li, *J. Lumin.* **122–123**, 707–709 (2007)